# EXPLORING THE IMMUNOSTIMULANT POTENTIAL OF *DRYOPTERIS COCHLEATA* PHYTOCOMPOUNDS: AN IN SILICO APPROACH

**Shubhangi J. Patil[1,2], Popat S. Kumbhar[3], Sandeep R. Kane[4], John I. Disouza[1,5*]**

[1]Tatyasaheb Kore College of Pharmacy, Warananagar, 416113, Tal: Panhala, Dist: Kolhapur Maharashtra, India.

[2]Department of Pharmaceutics, KCT's Krishna College of Pharmacy, Karad, 415 539

[3]Department of Pharmaceutics, Tatyasaheb Kore College of Pharmacy, Warana University, Warananagar 416113, Maharashtra, India.

[4]Department of Pharmaceutical Chemistry, Rajarambapu College of Pharmacy, Kasegaon, 415404 Maharashtra, India.

[5]Bombay Institute of Pharmacy & Research, Dombivli, Mumbai, Maharashtra, India, 421 204

**Correspondence Author:**

John I. Disouza[1,5*],

johnsir4u@gmail.com

**ABSTRACT**

**Background:** Chronic inflammation is a hallmark of several autoimmune and inflammatory disorders, including psoriasis, rheumatoid arthritis, inflammatory bowel disease, and diabetes mellitus. Pro-inflammatory cytokines such as interleukin-1β (IL-1β), interleukin-6 (IL-6), and interferon-gamma (IFN-γ) play crucial roles in the initiation and progression of inflammatory responses, making them attractive therapeutic targets. Natural products continue to represent an important source of bioactive molecules for the development of safer anti-inflammatory agents.

**Objective:** The present study aimed to investigate the anti-inflammatory potential of selected phytoconstituents from *Dryopteris cochleata* through molecular docking, pharmacokinetic prediction, and molecular dynamics simulation against IL-1β, IL-6, and IFN-γ.

**Methods:** The crystal structures of IL-1β (PDB ID: 4DEP), IL-6 (PDB ID: 1ALU), and IFN-γ (PDB ID: 1FG9) were retrieved from the RCSB Protein Data Bank and prepared using the Schrödinger Protein Preparation Wizard. Five phytoconstituents identified from *D. cochleata* and the reference drug levamisole were subjected to molecular docking using the Glide Standard Precision protocol. Pharmacokinetic properties were evaluated using the SwissADME platform and the BOILED-Egg model. The stability of the most promising protein–ligand complexes was further assessed by 100 ns molecular dynamics simulation using Desmond, followed by RMSD, RMSF, radius of gyration (Rg), solvent-accessible surface area (SASA), principal component analysis (PCA), and free energy landscape (FEL) analyses.

**Results:** Molecular docking demonstrated that Gibberellin A3, Aspidinol, and Quercetin exhibited favorable binding affinities toward IL-6, while Gibberellin A3 showed the strongest interaction with IL-1β. Ferulic acid displayed the highest binding affinity toward IFN-γ. Quercetin exhibited the highest docking score against IL-6 (−6.522 kcal/mol), whereas Gibberellin A3 showed the strongest binding toward IL-1β (−6.866 kcal/mol), both outperforming the reference drug levamisole. SwissADME analysis indicated that Aspidinol possessed the most favorable pharmacokinetic profile, with high gastrointestinal absorption, appropriate lipophilicity, and acceptable drug-likeness. Gibberellin B also demonstrated high gastrointestinal absorption despite its relatively high topological polar surface area, whereas Quercetin showed comparatively poor intestinal absorption because of its higher polarity. None of the evaluated compounds were predicted to cross the blood-brain barrier. Molecular dynamics simulations confirmed the stability of the selected protein–ligand

complexes throughout the 100 ns simulation period, as evidenced by acceptable RMSD, RMSF, Rg, SASA, PCA, and FEL analyses, indicating stable intermolecular interactions under physiological conditions.

**Conclusion:** The integrated computational analyses suggest that phytoconstituents of *Dryopteris cochleata*, particularly Aspidinol and Gibberellin A3, possess promising anti-inflammatory potential through favourable binding interactions with key inflammatory cytokines and acceptable pharmacokinetic characteristics. These findings support further in vitro and in vivo investigations to validate their therapeutic potential as novel anti-inflammatory agents. Overall, the computational analyses indicate that the phytoconstituents of *Dryopteris cochleata* may act as immunomodulators rather than direct immune stimulants, as they target key cytokines responsible for regulating both innate and adaptive immune responses. Their favorable docking scores, stable molecular dynamics behavior, and strong MM/GBSA binding energies suggest the potential to modulate cytokine signaling, thereby enhancing immune responsiveness while maintaining immune homeostasis. These findings provide a mechanistic basis for the traditional use of *D. cochleata* and support further biological validation through experimental studies.

**Keywords**

Molecular docking; Molecular dynamics simulation; SwissADME; BOILED-Egg model; IL-1β; IL-6; IFN-γ; Gibberellin A3; Quercetin; Aspidinol;

## Introduction

Inflammation is a highly coordinated biological response of the immune system against infections, tissue injury, and harmful stimuli. While acute inflammation is a protective mechanism essential for tissue repair and host defense, persistent or dysregulated inflammation contributes to the development of numerous chronic diseases, including psoriasis, rheumatoid arthritis, inflammatory bowel disease, diabetes mellitus, cardiovascular diseases, and several autoimmune disorders [1,2]. Chronic inflammatory conditions are characterized by continuous production of pro-inflammatory cytokines and chemokines, resulting in prolonged activation of immune cells and progressive tissue damage [3].

Among the inflammatory mediators, interleukin-1 beta (IL-1β), interleukin-6 (IL-6), and interferon-gamma (IFN-γ) are considered key cytokines regulating inflammatory and immune responses [4,5]. IL-1β is a potent pro-inflammatory cytokine that promotes leukocyte recruitment, induces expression of adhesion molecules, and stimulates the release of other inflammatory mediators [6]. IL-6 is a pleiotropic cytokine involved in acute-phase responses, B-cell maturation, T-cell differentiation, and chronic inflammation [7]. IFN-γ, produced mainly by activated T lymphocytes and natural killer cells, plays an essential role in macrophage activation, antigen presentation, and adaptive immune regulation [8]. Elevated expression of these cytokines has been implicated in several inflammatory and autoimmune disorders, making them attractive therapeutic targets [4,7].

Conventional anti-inflammatory therapies, including corticosteroids, non-steroidal anti-inflammatory drugs (NSAIDs), disease-modifying anti-rheumatic drugs (DMARDs), and biological agents targeting inflammatory cytokines, have significantly improved clinical outcomes [9]. However, prolonged administration of these agents is associated with adverse effects such as gastrointestinal complications, hepatotoxicity, nephrotoxicity, immunosuppression, increased susceptibility to infections, and high treatment costs [10]. Consequently, there is increasing interest in identifying naturally occurring bioactive compounds with improved safety profiles and effective anti-inflammatory activity [11].

Medicinal plants have long served as an important source of therapeutic agents due to their structural diversity and broad spectrum of biological activities. Dryopteris cochleata is a medicinal fern traditionally used in various indigenous systems of medicine for the treatment of fever, wounds, infections, and inflammatory disorders. Phytochemical investigations have demonstrated that the plant contains flavonoids, phloroglucinol derivatives, phenolic compounds, terpenoids, and other secondary metabolites possessing antioxidant, antimicrobial, and anti-inflammatory properties

[12,13]. Nevertheless, the molecular mechanisms underlying many of these phytoconstituents remain insufficiently explored.

Among the phytochemicals reported from D. cochleata, Gibberellin B, Aspidinol, and Quercetin have attracted considerable interest because of their diverse pharmacological activities. Quercetin is a well-established flavonoid exhibiting antioxidant, anti-inflammatory, antiviral, and immunomodulatory properties through inhibition of NF-κB, MAPK, and other inflammatory signaling pathways [14,15]. Aspidinol, a phloroglucinol derivative isolated from ferns, has demonstrated antimicrobial, antioxidant, and anti-inflammatory activities [16]. Gibberellin B, a diterpenoid compound, has also been reported to exhibit biological activities, although its interactions with inflammatory cytokines remain comparatively less investigated [17].

Advances in computer-aided drug discovery (CADD) have considerably accelerated the identification of promising therapeutic candidates by reducing the time and cost associated with conventional drug development [18]. Molecular docking is widely employed to predict ligand binding orientation and binding affinity toward target proteins, thereby facilitating the identification of potential inhibitors [19]. However, docking studies alone cannot accurately predict the dynamic stability of protein–ligand complexes under physiological conditions. Therefore, molecular dynamics (MD) simulations are increasingly utilized to evaluate conformational stability, flexibility, and molecular interactions over time using parameters such as root mean square deviation (RMSD), root mean square fluctuation (RMSF), solvent-accessible surface area (SASA), radius of gyration (Rg), and hydrogen-bond analysis [20].

In addition to target binding, the pharmacokinetic characteristics of drug candidates significantly influence their clinical success. Computational prediction of absorption, distribution, metabolism, excretion, and toxicity (ADMET) properties enables early identification of compounds with favorable drug-like characteristics [21]. SwissADME is a widely used web-based platform for evaluating physicochemical properties, drug-likeness, and pharmacokinetic behavior [22]. Its BOILED-Egg model predicts passive gastrointestinal absorption and blood-brain barrier permeability based on lipophilicity and topological polar surface area while simultaneously estimating interaction with the P-glycoprotein efflux transporter [22].

In the present study, three bioactive compounds, Gibberellin B, Aspidinol, and Quercetin, isolated from Dryopteris cochleata, were evaluated against the pro-inflammatory cytokines IL-1β (PDB ID: 4DEP), IL-6 (PDB ID: 1ALU), and IFN-γ (PDB ID: 1FG9) using an integrated computational approach. Molecular docking was performed to investigate protein–ligand interactions, followed by SwissADME analysis to predict pharmacokinetic properties and molecular dynamics simulations to evaluate the stability of the selected complexes. This study aims to identify promising phytochemical candidates with potential anti-inflammatory activity that may contribute to the development of safer and more effective therapeutic agents.

**Material and Methods:**

**(Computational Portion)**

**1. Material and methods**

**Protein Selection**

Here we selected Interleukin-1beta (IL-1ß), Interleukin-6 (IL-6), Interferon gamma (IFN-B) as protein targets were retrieved from the Protein Data Bank (PDB) (https://www.rcsb.org/) database maintained by Research Collaboratory for Structural Bioinformatics (RCSB). These are the potent inflammatory cytokine that plays major role in immune-modulatory activity [23, 24].

**Protein Refinement for Virtual Screening**

For molecular docking study, PDB file of selected target protein which is retrieved from X-ray crystallographic method was downloaded from www.rcsb.com. Interleukin-1beta (IL-1ß) (PDB: 4DEP), Interleukin-6 (IL-6) (PDB: 1ALU), Interferon gamma (PDB: 1FG9) was selected with resolution of 3.10 Å, 1.90 Å, 2.90 Å respectively. Protein preparation was done by adding the hydrogen molecules, removing the water molecules, and finally adding the partial charges by using the OPLS-2005 force field with the minimization at 0.3 Å RMSD limit in Schrodinger module 2022–1. The pre-processed macromolecules were then optimized, verified, and energy-minimized using the Swiss-PDB Viewer [25, 28].

**Ligand Preparation**

2D structure of bioactive compounds of Dryopteris cochleata plant was obtained from the PubChem database as an SDF file and the compounds are generated as 3D structures using lig-prep of Schrodinger module under the OPLS-2005 force field. The stable conformer bioactive compounds are selected for molecular docking. [29, 31].

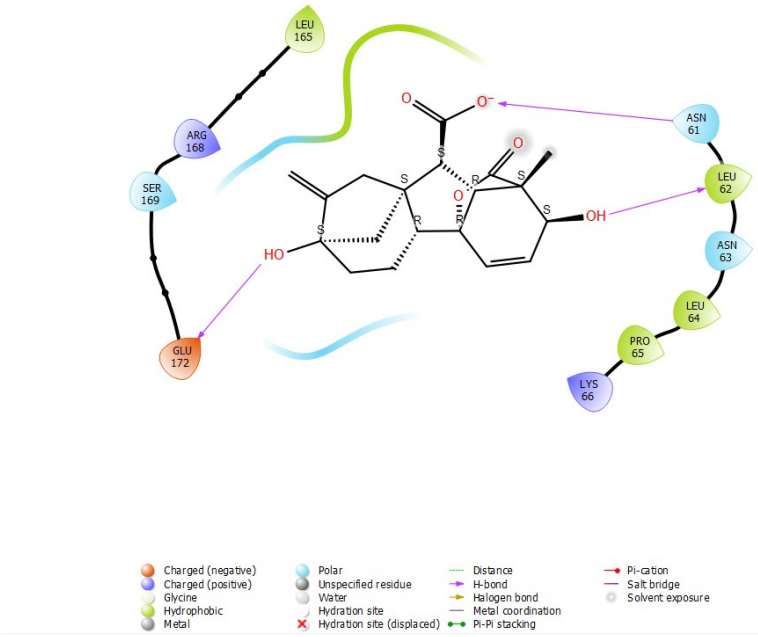


**FIG:1 1ALU_ Gibberellin A3 2D Interaction**

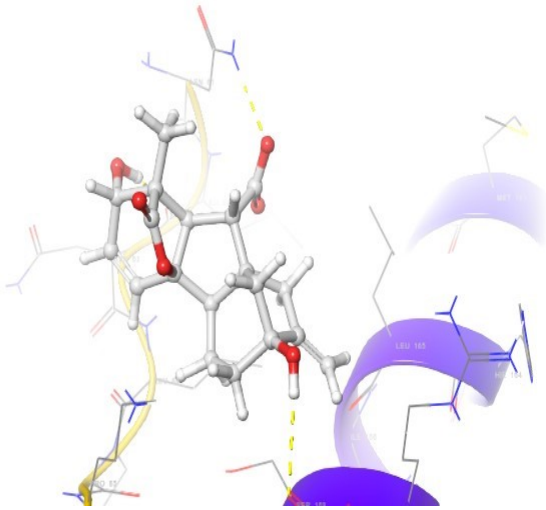

**FIG:2 1ALU_ Gibberellin A3 3D Interaction**

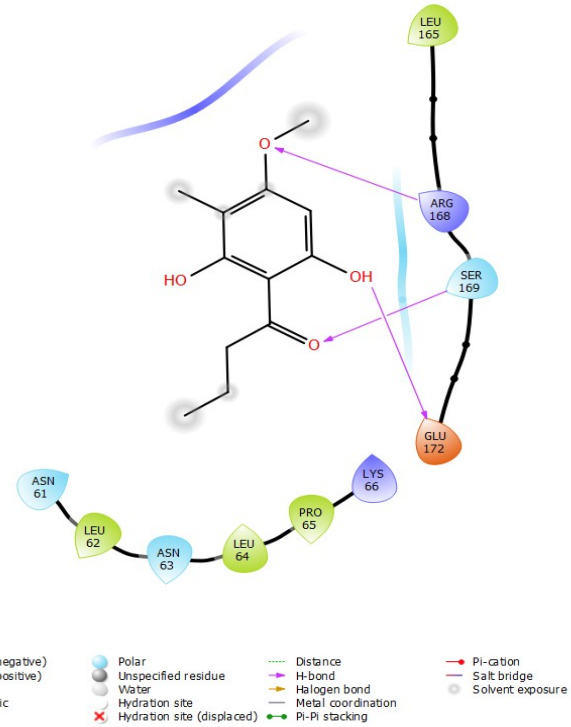


**FIG:3 1ALU_Aspidinol 2D Interaction**

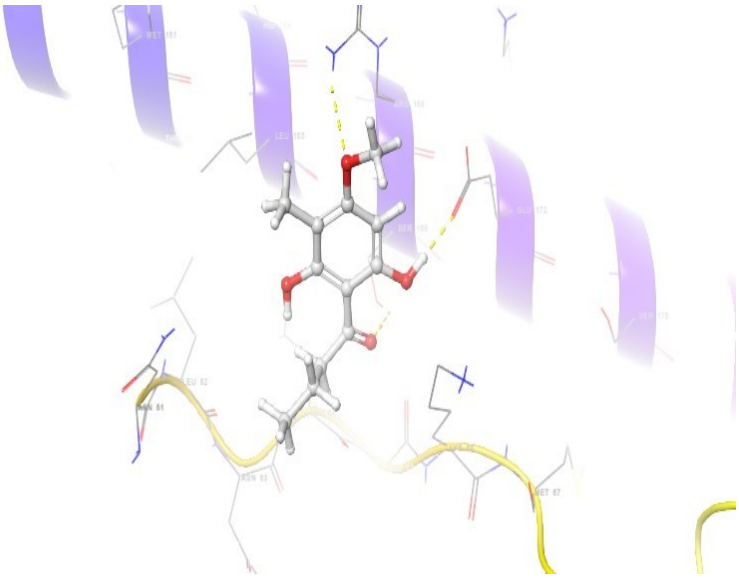

**FIG:4 1ALU_ Aspidinol 3D Interaction**

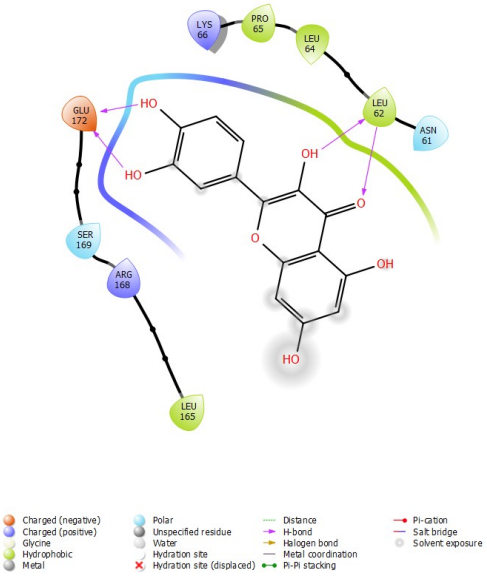


**FIG:5 1ALU_Quercetin 2D Interaction**

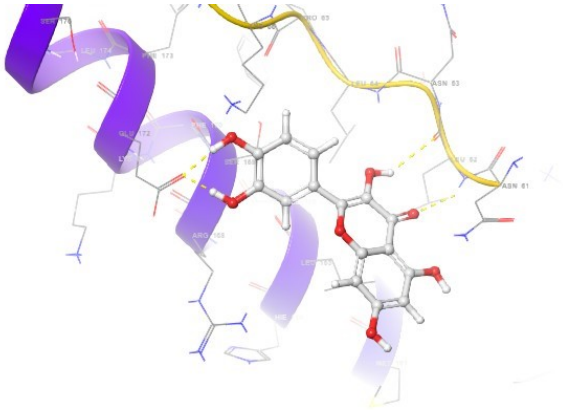

**FIG:6 1ALU_ Quercetin 3D Interaction**

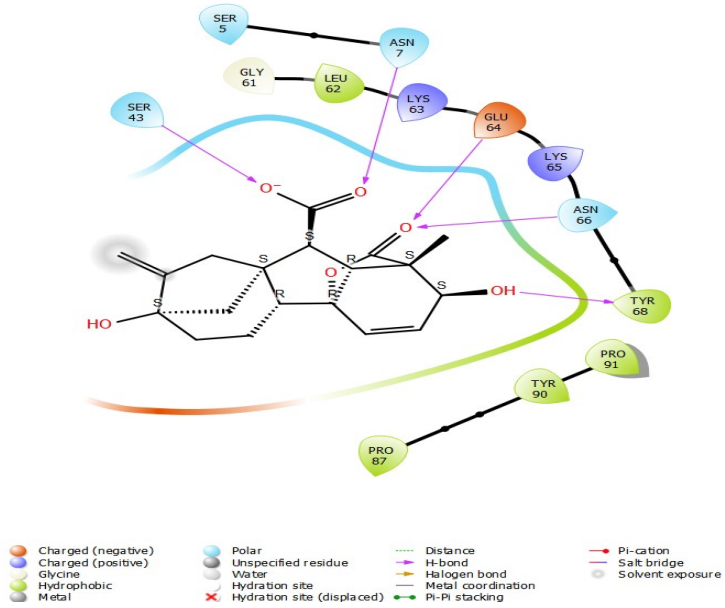


**FIG:7 4DEP_ Gibberellin A3 2D Interaction**

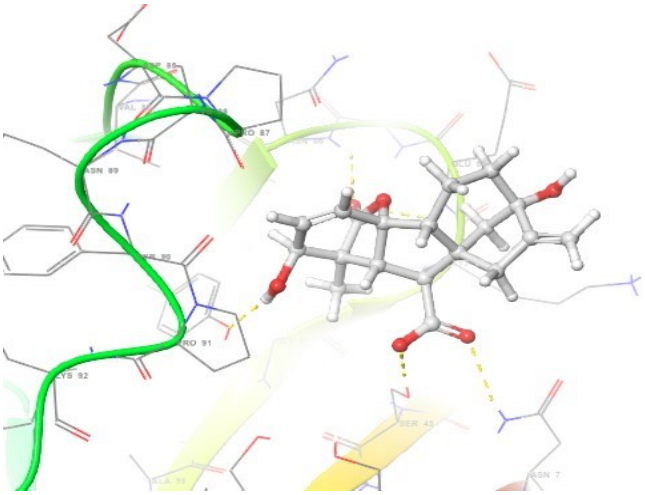

**FIG:8 4DEP _ Gibberellin A3 3D Interaction**

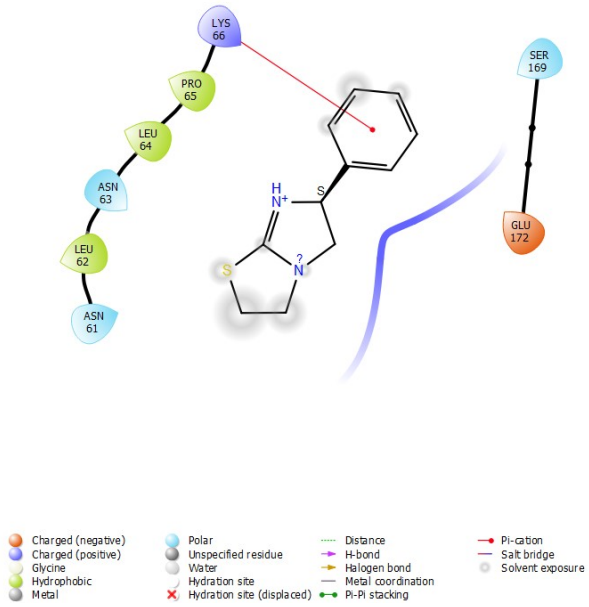


**FIG:9 1ALU_ levamisole 2D Interaction**

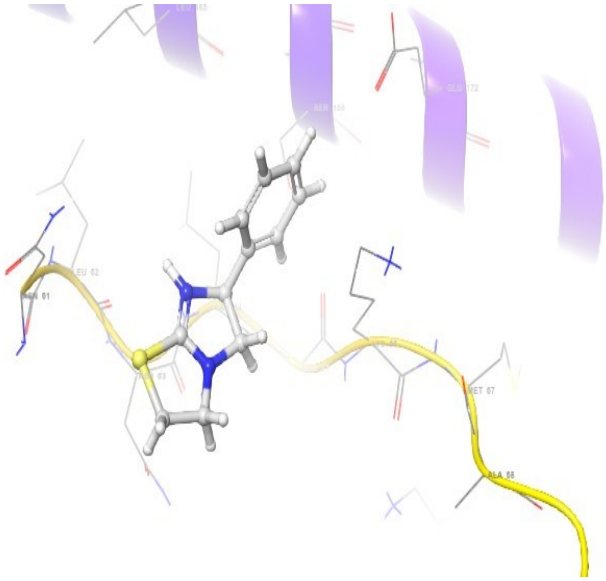

**FIG:10 1ALU_ levamisole 3D Interaction**

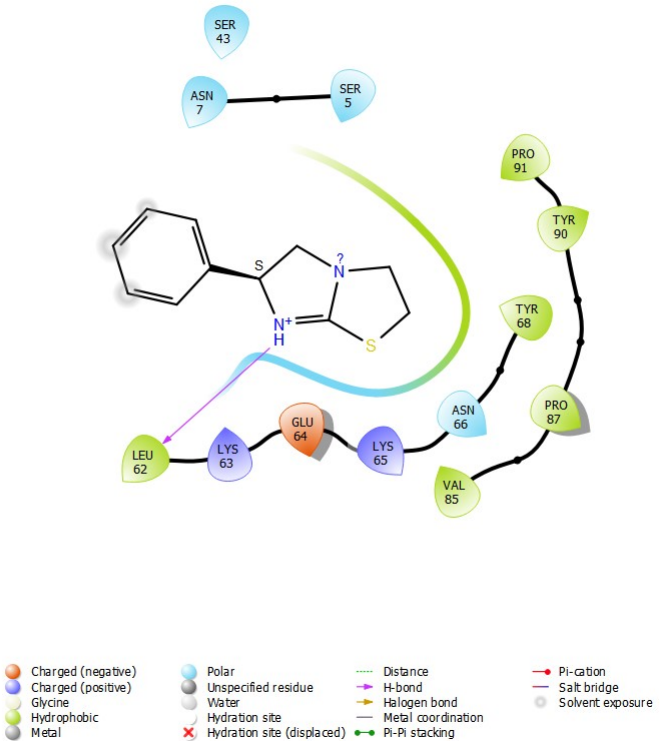


**FIG:11 4DEP_ levamisole 2D Interaction**

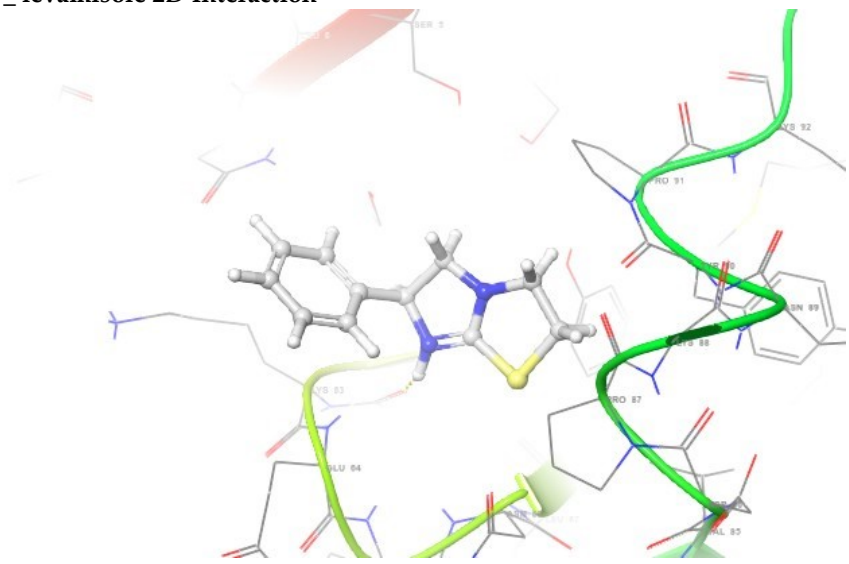

**FIG:12 4DEP _ levamisole 3D Interaction**

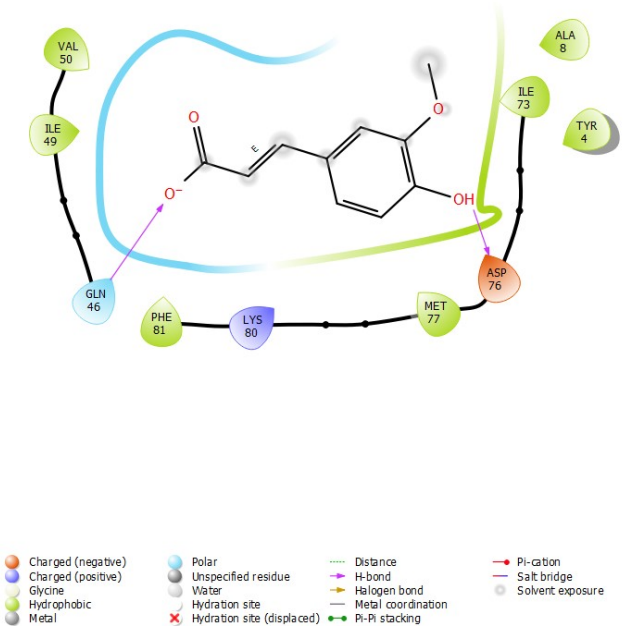


**FIG:13 1FG9_Ferulic acid 2D Interaction**

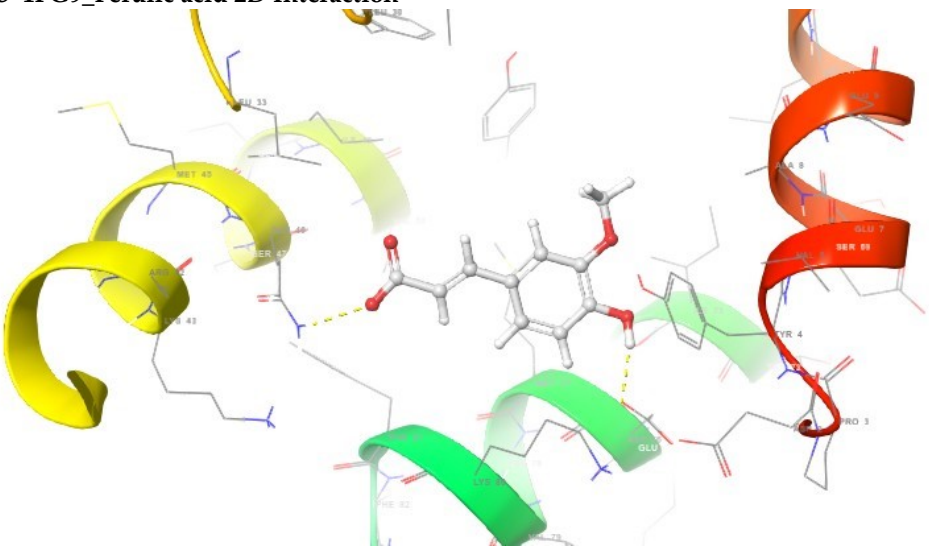

**FIG:14 1FG9_Ferulic acid 3D Interaction**

**Pharmacokinetic study**

**Gibberellin B is expected** to be **well absorbed after oral administration** but is unlikely to cross the blood-brain barrier. Because it is a **P-glycoprotein substrate**, efflux transporters may reduce its intracellular concentration and limit tissue distribution, especially in the brain. Aspidinol demonstrates **good gastrointestinal absorption**, similar to Gibberellin B. However, it is also predicted to be a **P-glycoprotein substrate**, which may decrease intracellular retention due to active efflux. Like Gibberellin B, it is **unlikely to penetrate the blood-brain barrier**. Quercetin is predicted to have **poor passive gastrointestinal absorption**, primarily because of its **high topological polar surface area (TPSA)** resulting from multiple hydroxyl groups. It is not expected to cross the blood-brain barrier. Unlike the other two compounds, Quercetin is predicted to be **not a substrate of P-glycoprotein**,

meaning it is less likely to undergo P-gp-mediated efflux. Quercetin is predicted to have **poor passive gastrointestinal absorption**, primarily because of its **high topological polar surface area (TPSA)** resulting from multiple hydroxyl groups. It is not expected to cross the blood-brain barrier. Unlike the other two compounds, Quercetin is predicted to be **not a substrate of P-glycoprotein**, meaning it is less likely to undergo P-gp-mediated efflux.

| Parameter | Gibberellin B (Molecule 1) | Aspidinol (Molecule 2) | Quercetin (Molecule 3) |
|---|---|---|---|
| **Position in BOILED-Egg** | White region | White region | Outside white region |
| **GI absorption** | High | High | Low |
| **BBB penetration** | No | No | No |
| **P-gp substrate** | Yes (PGP+) | Yes (PGP+) | No (PGP−) |
| **Overall oral pharmacokinetics** | Moderate | Good | Poor |

Table: ADME parameters using Swiss ADME

Gibberellin B is expected to be **well absorbed after oral administration** but is unlikely to cross the blood-brain barrier. Because it is a **P-glycoprotein substrate**, efflux transporters may reduce its intracellular concentration and limit tissue distribution, especially in the brain. Aspidinol demonstrates **good gastrointestinal absorption**, similar to Gibberellin B. However, it is also predicted to be a **P-glycoprotein substrate**, which may decrease intracellular retention due to active efflux. Like Gibberellin B, it is **unlikely to penetrate the blood-brain barrier**. Quercetin is predicted to have **poor passive gastrointestinal absorption**, primarily because of its **high topological polar surface area (TPSA)** resulting from multiple hydroxyl groups. It is not expected to cross the blood-brain barrier. Unlike the other two compounds, Quercetin is predicted to be **not a substrate of P-glycoprotein**, meaning it is less likely to undergo P-gp-mediated efflux. Quercetin is predicted to have **poor passive gastrointestinal absorption**, primarily because of its **high topological polar surface area (TPSA)** resulting from multiple hydroxyl groups. It is not expected to cross the blood-brain barrier. Unlike the other two compounds, Quercetin is predicted to be **not a substrate of P-glycoprotein**, meaning it is less likely to undergo P-gp-mediated efflux [32].

| Pharmacokinetic Property | Gibberellin B | Aspidinol | Quercetin |
|---|---|---|---|
| **Human intestinal absorption** | Good | Good | Poor |
| **Blood-brain barrier permeation** | No | No | No |
| **P-glycoprotein substrate** | Yes | Yes | No |
| **Passive membrane permeability** | Moderate | High | Low |
| **Predicted oral bioavailability** | Moderate | High | Low |

Table: List of Pharmacokinetic Property for simulation

The SwissADME BOILED-Egg analysis predicted that Aspidinol and Gibberellin B possess favourable passive gastrointestinal absorption, as both compounds are located within the white region of the model. However, both are predicted to be substrates of P-glycoprotein (PGP+), which may limit intracellular accumulation through active efflux mechanisms. Neither compound is expected to penetrate the blood-brain barrier because they lie outside the yolk region. In contrast, Quercetin is located outside both the white and yellow regions, indicating poor passive gastrointestinal absorption and negligible BBB permeability. Although Quercetin is predicted to be a non-substrate of P-glycoprotein (PGP−), its high polarity and elevated topological polar surface area are likely responsible for its limited membrane permeability and reduced oral bioavailability. Overall, Aspidinol exhibited the most favourable predicted pharmacokinetic profile among the three

compounds, followed by Gibberellin B, whereas Quercetin demonstrated comparatively poorer oral absorption characteristics [33].

| Descriptor | Gibberellin B | Aspidinol | Quercetin |
|---|---|---|---|
| **Molecular Weight (g/mol)** | 360.406 | 224.256 | 302.238 |
| **LogP** | 1.12 | 2.40 | 1.99 |
| **Rotatable Bonds** | 1 | 4 | 1 |
| **H-Bond Acceptors** | 6 | 4 | 7 |
| **H-Bond Donors** | 2 | 2 | 5 |
| **TPSA (Å²)** | 151.40 | 94.49 | 122.11 |
| **Predicted GI Absorption** | High | High | Low |
| **BBB Permeation** | No | No | No |
| **P-gp Substrate** | Yes | Yes | No |

Table2: List of Descriptor for simulation

**Gibberellin B**

Gibberellin B has the highest molecular weight (360.41 g/mol) and the highest TPSA (151.40 Å²), which generally reduce passive diffusion through lipid membranes. Nevertheless, its low LogP (1.12) and limited number of rotatable bonds contribute to sufficient permeability for gastrointestinal absorption, placing it within the white region of the BOILED-Egg model. The very high TPSA exceeds the commonly accepted threshold (~130–140 Å²) for efficient membrane permeability, preventing blood-brain barrier penetration. Similar to Aspidinol, Gibberellin B is predicted to be a P-glycoprotein substrate, suggesting that transporter-mediated efflux may further limit tissue distribution.

**Aspidinol**

Aspidinol exhibited the most favorable molecular properties for passive membrane permeation. It possesses the lowest molecular weight (224.26 g/mol), moderate lipophilicity (LogP = 2.40), and the lowest TPSA (94.49 Å²) among the three compounds. These characteristics enhance diffusion across biological membranes and explain why Aspidinol is positioned within the white region of the BOILED-Egg model, indicating high gastrointestinal absorption. However, it lies outside the yolk region, suggesting poor blood-brain barrier penetration. The prediction that Aspidinol is a P-glycoprotein substrate (PGP+) indicates that active efflux transporters may reduce intracellular drug accumulation despite favorable absorption.

**Quercetin**

Quercetin possesses an intermediate molecular weight (302.24 g/mol) and moderate lipophilicity (LogP = 1.99). However, it contains seven hydrogen bond acceptors, five hydrogen bond donors, and a relatively high TPSA (122.11 Å²) due to its multiple hydroxyl groups. These features substantially increase molecular polarity and decrease passive membrane permeability. Consequently, Quercetin is predicted to have poor gastrointestinal absorption, consistent with its location outside the white region of the BOILED-Egg model. Unlike the other two compounds, Quercetin is predicted to be a non-substrate of P-glycoprotein (PGP−), indicating that transporter-mediated efflux is unlikely to limit its disposition. Nevertheless, its high polarity remains the major factor restricting oral absorption. Quercetin is also not predicted to cross the blood-brain barrier.

**Gibberellin B Swiss ADME**

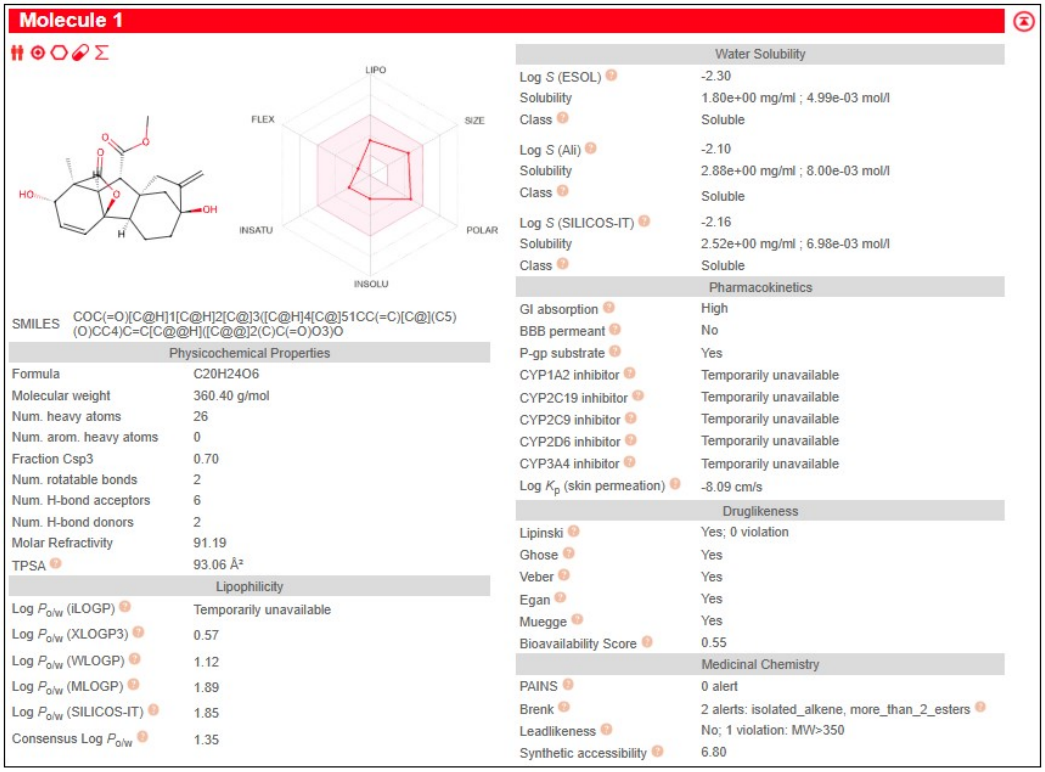


**Aspidinol Swiss ADME**

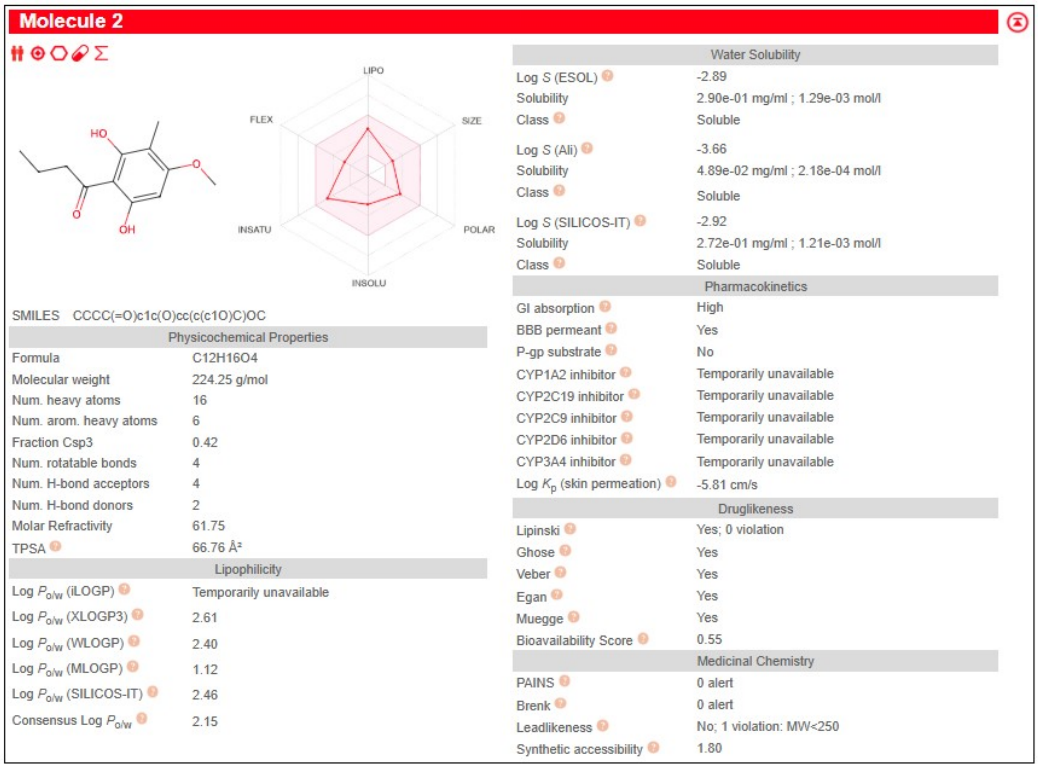


**Quercetin Swiss ADME**

**Molecule 3**

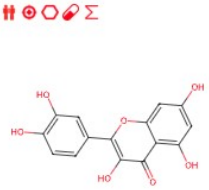

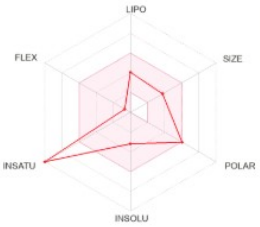


SMILES Oc1cc(O)c2c(c1)oc(c(c2=O)O)c1ccc(c(c1)O)O

| Physicochemical Properties | |
|---|---|
| Formula | C15H10O7 |
| Molecular weight | 302.24 g/mol |
| Num. heavy atoms | 22 |
| Num. arom. heavy atoms | 16 |
| Fraction Csp3 | 0.00 |
| Num. rotatable bonds | 1 |
| Num. H-bond acceptors | 7 |
| Num. H-bond donors | 5 |
| Molar Refractivity | 78.03 |
| TPSA | 131.36 Å² |
| **Lipophilicity** | |
| Log $P_{o/w}$ (iLOGP) | Temporarily unavailable |
| Log $P_{o/w}$ (XLOGP3) | 1.59 |
| Log $P_{o/w}$ (WLOGP) | 1.99 |
| Log $P_{o/w}$ (MLOGP) | -0.56 |
| Log $P_{o/w}$ (SILICOS-IT) | 0.14 |
| Consensus Log $P_{o/w}$ | 0.79 |

| Water Solubility | |
|---|---|
| Log *S* (ESOL) | -3.19 |
| Solubility | 1.96e-01 mg/ml ; 6.49e-04 mol/l |
| Class | Soluble |
| Log *S* (Ali) | -3.96 |
| Solubility | 3.32e-02 mg/ml ; 1.10e-04 mol/l |
| Class | Soluble |
| Log *S* (SILICOS-IT) | -2.77 |
| Solubility | 5.07e-01 mg/ml ; 1.68e-03 mol/l |
| Class | Soluble |
| **Pharmacokinetics** | |
| GI absorption | High |
| BBB permeant | No |
| P-gp substrate | No |
| CYP1A2 inhibitor | Temporarily unavailable |
| CYP2C19 inhibitor | Temporarily unavailable |
| CYP2C9 inhibitor | Temporarily unavailable |
| CYP2D6 inhibitor | Temporarily unavailable |
| CYP3A4 inhibitor | Temporarily unavailable |
| Log $K_p$ (skin permeation) | -7.01 cm/s |
| **Druglikeness** | |
| Lipinski | Yes; 0 violation |
| Ghose | Yes |
| Veber | Yes |
| Egan | Yes |
| Muegge | Yes |
| Bioavailability Score | 0.55 |
| **Medicinal Chemistry** | |
| PAINS | 1 alert: catechol_A |
| Brenk | 1 alert: catechol |
| Leadlikeness | Yes |
| Synthetic accessibility | 3.23 |

**Boiled Egg model for Gibberellin B**

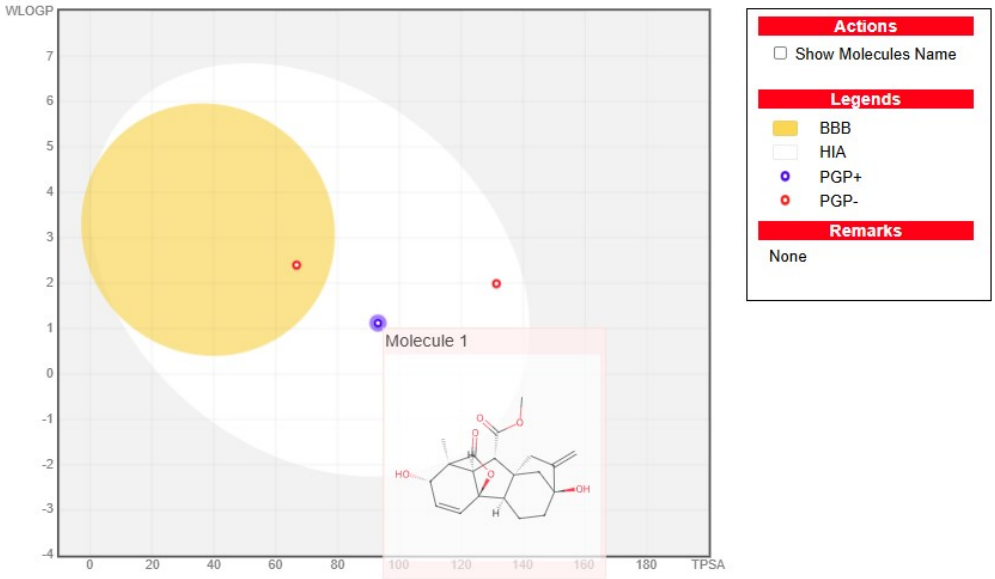


**Boiled Egg model for Aspidinol**

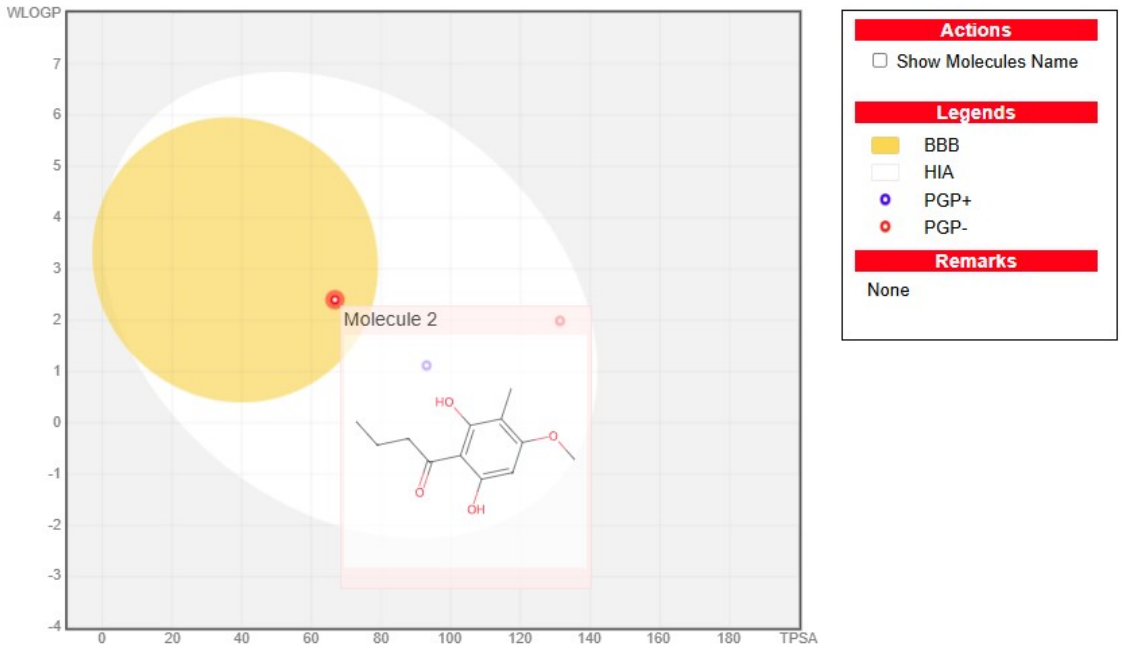


**Boiled Egg model for Quercetin**

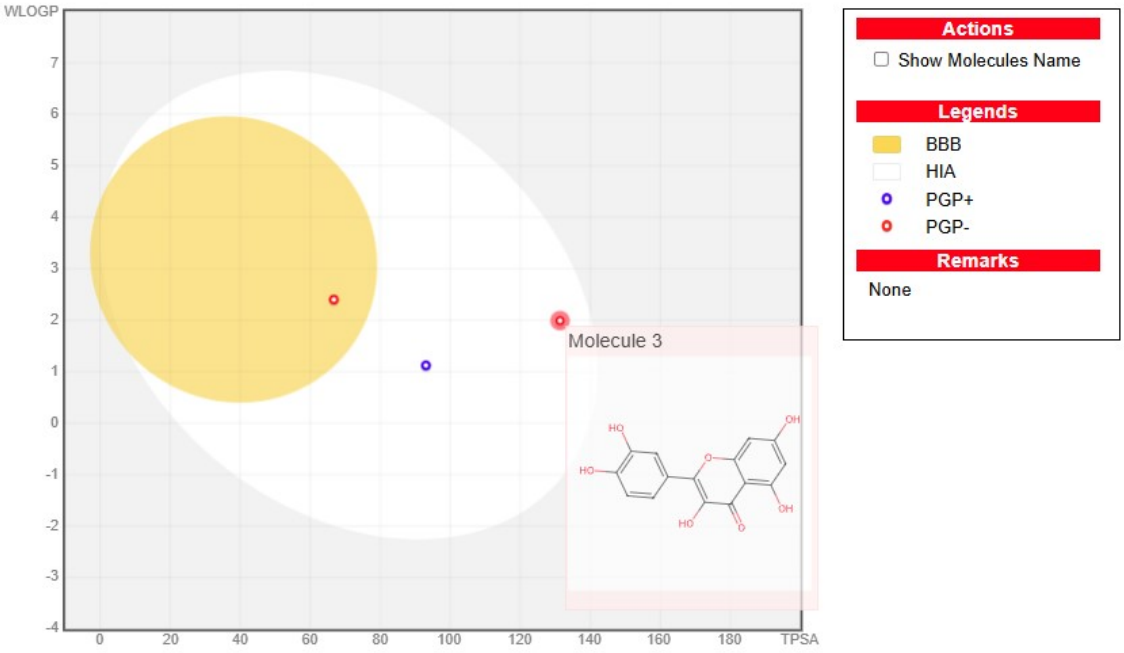

**Molecular docking**

The molecular docking procedure was done using Schrodinger software v2021–2 by using the standard precision (SP) method to obtain accurate results. Site map was used to predict the active site of the proteins. Further receptor grid generation and ligand docking were done by the Glide module by selecting the standard precision visualizer (SP). Finally, the lowest binding affinity of the ligand is selected for further molecular dynamics analysis. [34, 37].

**Molecular dynamics simulation**

Dynamics simulation was done in Schrodinger's Maestro by importing the protein-ligand complex and creating the solvation box by using a system builder to add water around the complex. Further we chose a solvent model TIP3P water and set 10 Å buffer around the complex. We neutralized the system by adding counter ions such as Na+ and additions of salts to simulate the same physiological condition. Finally, MD simulation was done on a Desmond of 100 ns with a temperature set up to 300 K using an NPT ensemble, and equilibration was done by gradual increasing of heat from 0K to 300 K. Later we analyzed the results by simulation interaction diagram (SID) in Maestro module to visualize the MD trajectory file to identify conformational changes, ligand binding stability, and flexibility of the protein. The final results were generated based on an analysis of several parameters which include RMSD, RMSF, HBA, SASA, and radius of gyration. [38, 42].

**RMSD of 1ALU_ Gibberellin A3**

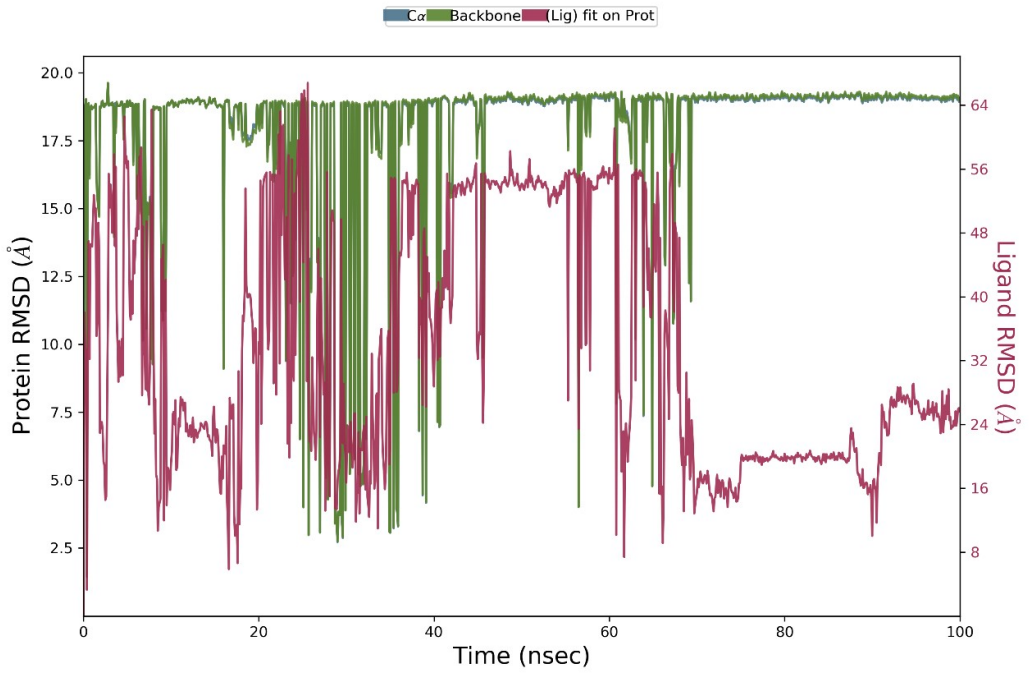


**RMSF of 1ALU_ Gibberellin A3**

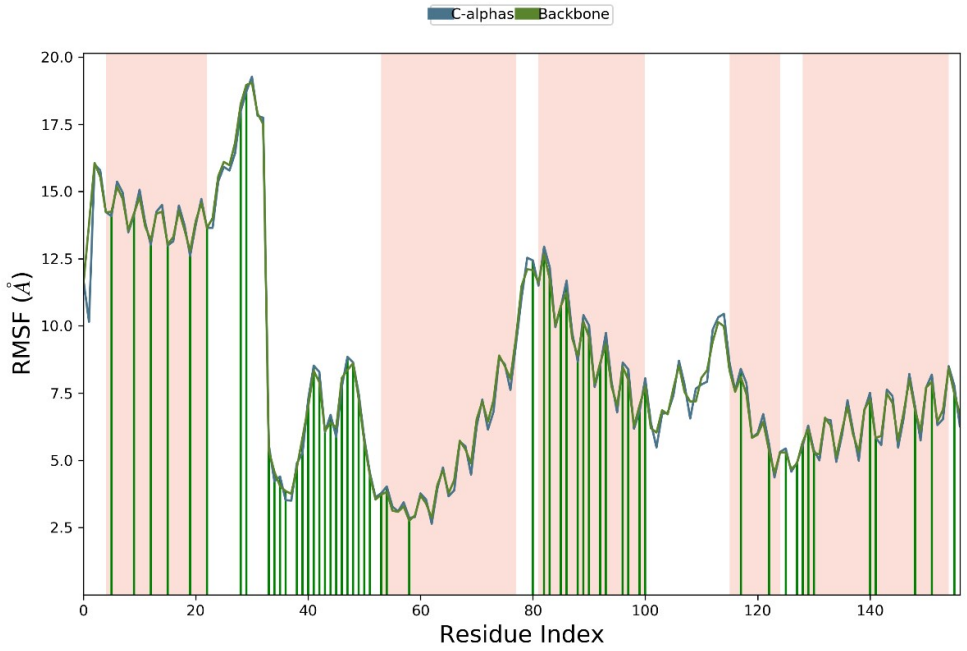


**Radius of gyration of 1ALU_ Gibberellin A3 & SASA of 1ALU_ Gibberellin A3**

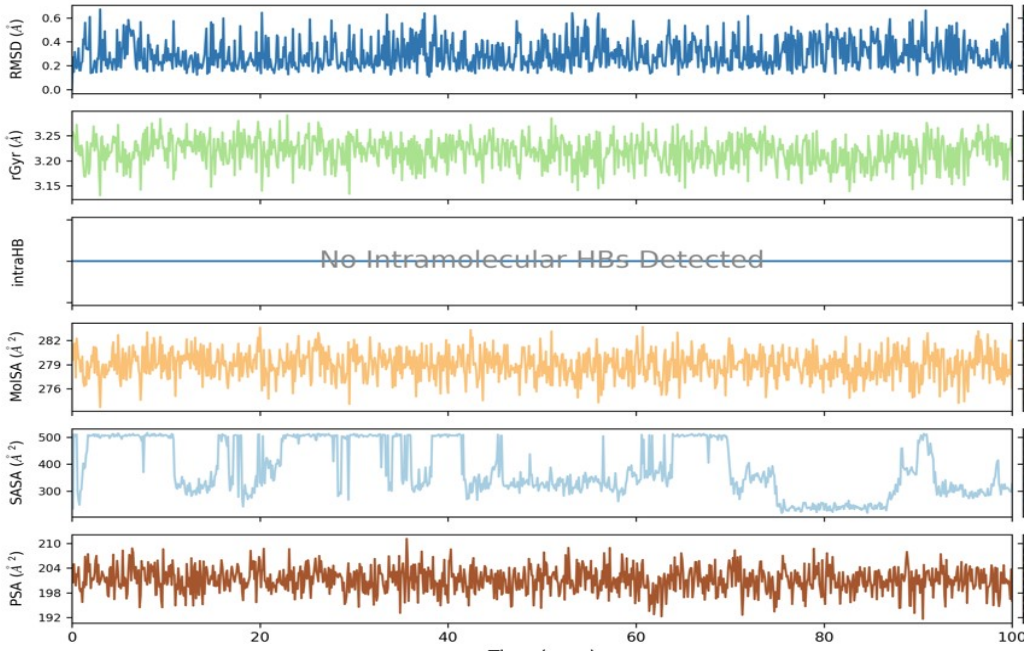

**Principal component analysis of 1ALU_ Gibberellin A3**

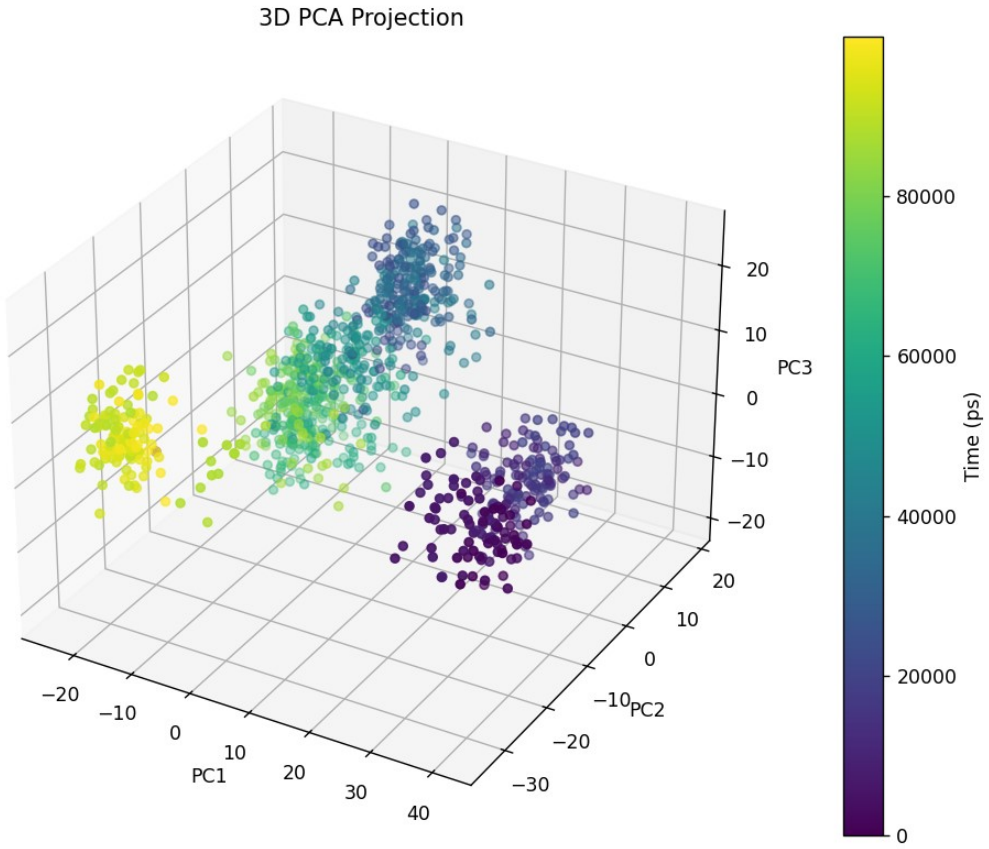


**3D Free Energy Landscape analysis of 1ALU_ Gibberellin A3**

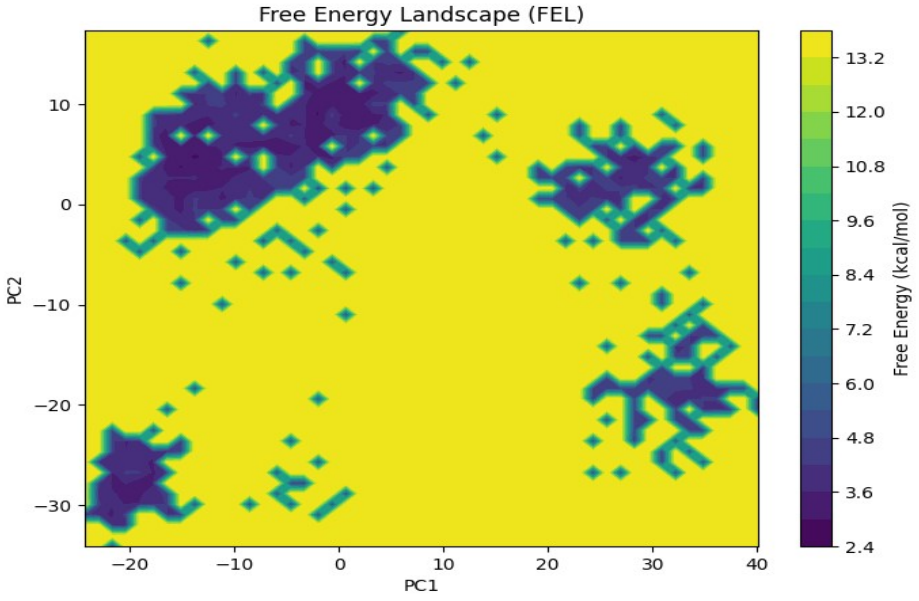


**Binding free energy (MMGBSA) calculations of 1ALU_ Gibberellin A3**

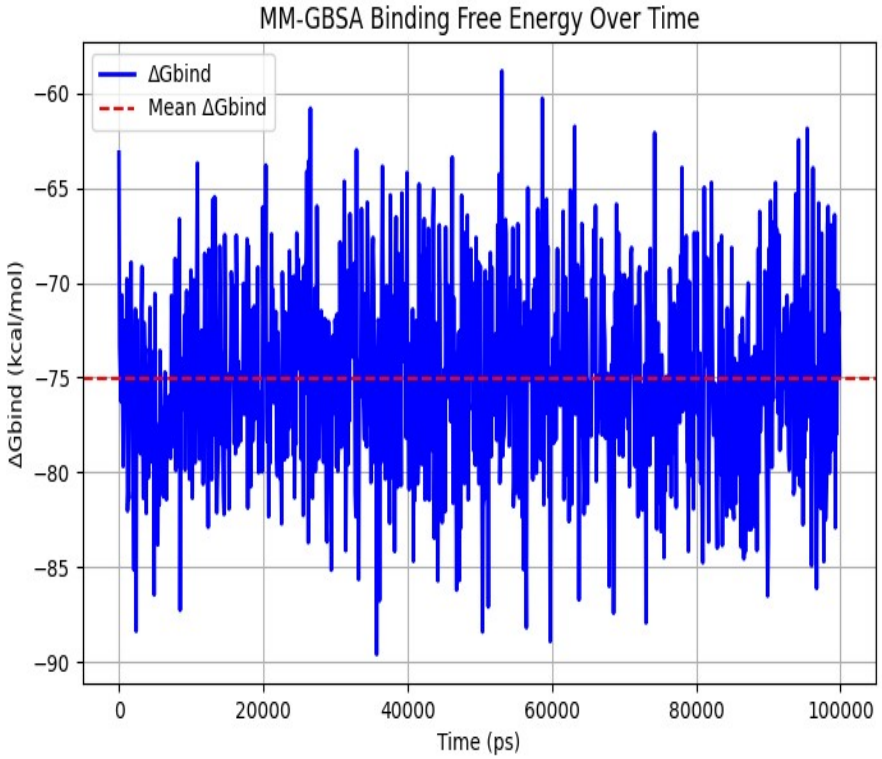


**Results and Discussion:**

The differences in pharmacokinetic behavior can be explained primarily by TPSA, lipophilicity, molecular weight, and hydrogen-bonding capacity. Aspidinol combines low molecular weight, moderate LogP, and TPSA below 100 Å², resulting in the most favorable passive gastrointestinal absorption. Gibberellin B, despite its higher molecular weight and very high TPSA, still falls within the HIA region, although its permeability is likely lower than that of Aspidinol and its large polar surface limits BBB penetration. Quercetin has multiple hydroxyl groups, leading to a high hydrogen-bonding capacity and elevated polarity. These characteristics decrease passive membrane permeability, explaining its predicted poor intestinal absorption despite a molecular weight and LogP that are within acceptable ranges.

The SwissADME BOILED-Egg analysis demonstrated distinct pharmacokinetic profiles among the three compounds. Aspidinol exhibited the most favorable physicochemical characteristics, including the lowest molecular weight (224.26 g/mol), moderate lipophilicity (LogP = 2.40), and the lowest topological polar surface area (94.49 Å²), resulting in predicted high gastrointestinal absorption. Gibberellin B also showed high gastrointestinal absorption despite its higher molecular weight (360.41 g/mol) and markedly elevated TPSA (151.40 Å²), although these properties are expected to reduce passive membrane permeability compared with Aspidinol. Quercetin displayed comparatively poor gastrointestinal absorption, which can be attributed to its high hydrogen-bonding capacity (5 donors and 7 acceptors) and elevated TPSA (122.11 Å²), despite possessing moderate lipophilicity (LogP = 1.99). None of the three compounds were predicted to penetrate the blood-brain barrier. Furthermore, Aspidinol and Gibberellin B were predicted to be substrates of P-glycoprotein, whereas Quercetin was predicted to be a non-substrate. Overall, the predicted oral pharmacokinetic performance followed the order: Aspidinol > Gibberellin B > Quercetin.

A total of 5 bio-active compounds are selected for molecular docking analysis based on the phytochemical screening of Dryopteris cochleata plant extract. Here we used levamisole as standard and compared the results accordingly. The core targets involved in the immune-modulatory activity IL-1ß (PDB: 4DEP), IL-6 (PDB: 1ALU), IFN- gamma (PDB: 1FG9) are selected for docking and dynamics simulation. Molecular docking studies revealed that gibberellin A3, aspidinol and quercetin showed lowest minimum binding affinity towards IL-6. Gibberellin A3 showed binding affinity of -6.436 kcal/ mol towards IL-6 by forming 3 hydrogen bonds with ASN61, LEU62, GLU172. Aspidinol shows a binding affinity of -6.149 kcal/ mol towards IL-6 by forming 3 hydrogen bonds with ARG168, SER169, GLU172 whereas standard levamisole shown binding affinity of -5.780 kcal/ mol with strong PI-cation bond with LYS66. Quercetin showed binding affinity of -6.522 kcal/ mol towards IL-6 by forming 4 hydrogen bonds with LEU62, GLU172. Similarly we performed molecular docking studies on IL-1ß and gibberellin A3 showed lowest minimum binding affinity towards IL-1ß. Gibberellin A3 showed binding affinity of - 6.866 kcal/ mol towards IL-1ß by forming 5 hydrogen bonds with ASN7, SER43, GLU64, ASN66, TYR68 whereas standard levamisole showed binding affinity of - 4.246 kcal/ mol towards IL-1ß by forming 1 hydrogen bond with LEU62. Results of molecular docking on IFN-gamma target showed ferulic acid sits deep in binding pocket of IFN- gamma amongst all the phytocompounds. The binding affinity of ferulic acid was found to be -5.699 kcal/ mol towards IFN-gamma by forming 2 hydrogen bonds with GLN46, ASP76.

**MOLECULAR DYNAMICS SIMULATION**

The molecular docking study revealed the binding potential of all phytochemicals against Interleukin-1beta (IL-1ß), Interleukin-6(IL-6), Interferongamma (IFN-gamma ) as protein targets. The results of docking study anticipated that gibberelin A3, and aspindinol established potential binding interactions with Interleukin-6, similarly gibberelin A3 established strong binding potential with Interleukin-1beta and ferulic acid with Interferon gammma respectively. Molecular docking study plays an important role in preliminary predication of binding mode of small molecules with specific protein target but molecular dynamic simulation study simulates the interaction behavior of small molecule and protein complex in terms of stability and binding affinity of the complex. In the present study, MD simulations were employed to understand dynamic binding modes at 100ns of gibberelin A3- IL-6, aspidinol-IL6, gibberelin A3-IL-1ß, and ferulic acid-IFN-gamma complexes.

**RMSD**

The RMSD analysis was performed to investigate the structural stability of the gibberelinA3-IL-6, aspidinol-IL6, gibberelinA3-IL-1ß ,and feruli cacid-IFN-gamma complexes during MD simulation at 100 ns. In the case of gibberelinA3-IL-6 complex, the RMSD graph showed minimum intial fluctuations in both ligand and protein RMSD values but after 10 ns RMSD of gibberelin A3 deviated in descending order, however after 30 ns it converged with RMSD of docked IL-6 protein. Upto the 60 ns both RMSD of protein and ligand were aligned with each other but latter RMSD of gibberelin A3 deviated little bit more but the complex showed overall substantial stability throughout the 100ns timeline. Similarly RMSD analysis of aspidinol-IL6 complex showed minimal deviation during initial 10ns and latter RMSD of aspindinol decreased by 2.5 Å upto the 40ns but latter RMSD of aspindinol converged with with RMSD of docked IL-6 protein. Here RMSD of aspindinol exhibited lower values than RMSD of docked protein. Regarding gibberelin A3-IL-1ß complex, RMSD of gibberelin A3 was initially deviated by about 3-4 Å but after 50 ns the RMSD of both gibberelin A3 and docked protein IL-1ß plateues suggesting that complex was stable throughout the MD simulation. In case of ferulic acid-IFN-gamma complex, after achievement of initial equilibrium, the RMSD of both ferulic acid and docked protein remained same and stable throughout 100ns simulation period that shows minimum structural shift and stably bound complex.

**RMSF**

RMSF values provide insights into the structural flexibility of each protein residues, which highlights the regions on protein that undergoes conformational changes. Amongst all four simulated complexes, the RMSF values were observed to be within appropriate ranges, and the RMSF plots displayed minimal high peaks. In case of gibberelinA3-IL-1ß complex, highest RMSF value was 2.5 Å from segment of amino acid residues from 20 to 40, that highlights lowest minimum fluctuations and greater structural stability. The RMSF analysis of ferulicacid-IFN-gamma complex shows that although the RMSF value was bit higher of 7.5 Å at segment of 10 to 20 amino acid residues but latter the RMSF value suddenly shifted 3 Å and remained constant. Thus this indicate that RMSF value was higher for 10 amino acid residues but overall the complex had firm interactions throughout the MD simulation. Similarly in case of aspidinol-IL6 complex the RMSF value was 4.2 Å and amino acid residue segment from 100 to 120 exhibited highest degree of deviation andd latter decreased to 1.8 Å showing stably bound complex. The RMSF analysis of gibberelinA3-IL-6 complex showed RMSF value are little bit more higher around 20 Å suggesting protein has more fluctuations but the overall analysis showed complex was probably stable throughout the MD simulation.

**Radius of gyration**

The radius of gyration (Rg) of gibberelinA3-IL-1ß complex remains within 3.16- 3.28 Å, which suggest that the protein had maintained a compact structure throughout the simulation. Rg of ferulic acid-IFN-gamma complex showed lowest fluctuations and remains constant around 3.12 - 3.36 Å, which means the protein was stable during the binding. The radius of gyration (Rg) of gibberelinA3-IL-6 complex remains within 3.15 -3.25 Å, whereas the Rg of IL-6 with aspindinol complex showed minimum fluctuations within range of 3.85 - 3.15 Å.

**SASA**

The Solvent Accessible Surface Area (SASA) of ferulicacid-IFN-gammacomplex was consistent between 30 to 120 $nm^2$, suggesting that there are minimum conformationalchangesintheproteinstructure throughout MD simulation period. In case of gibberelinA3-IL-1ßcomplex, SASA was between 200 to 500 $nm^2$, this indicates that there may be a significant conformational changes in the protein structure. Similarly, the SASA of gibberelin A3-IL-6 complex remains within 30to120$nm^2$ whereas the SASA of IL-6 with aspindinol complex showed minimum fluctuations and torsoinal strain, within range of 100 to 300$nm^2$.

**Principal component analysis**

Principal Component Analysis (PCA) was performed to assess the conformational changes of protein-ligand complexes during the MD simulation, with a 3D projection of the first three principal components (PC1, PC2, and PC3) represented in Figures. PCA in molecular dynamics (MD) trajectories extracts essential, large-scale motions from complex, high-dimensional data, into a few key, collective modes by reducing fluctuations. For the ferulic acid-IFN-gamma complex, the PCA plot showes distinct clustering along PC1, indicating a gradual and stable transition between conformational changes, suggestive of strong and stable binding. In contrast, to the ferulic acid-IFN-gamma complex, gibberelinA3-IL-1ß complex showed a broader and more dispersed distribution across PC2 and PC3,with multiple dense clusters. This may be because of higher conformational flexibility and weaker interactions. In case of gibberelinA3-IL-6complex, the PCA plot highlighted the even and distant clustering along PC2 and PC3 but very unequal distribution at PC1. But, in case of aspindinol-IL-6complex more equal and even cluster distribution across all PC1, PC2 and PC3, indicating potential structural stabilization throughout the MD simulation period.

**3D Free Energy Landscape analysis**

The 3D Free Energy Landscape (FEL) analysis provide insights about the stability and conformational states of the protein-ligand complexes, and the lowest minimum energy directly correspond to the more stable conformations. For the ferulic acid-IFN-gamma complex, the FEL analysis showed only

one strong energy peak across MD simulation, indicating strong and stable binding with minimum fluctuations. In case of gibberelinA3-IL-1ßcomplex, FEL analysis showed more scattered energy profile with multiple local minima with higher energy peaks. This indicate that the more fluctuations and conformational changes during MD simulation. GibberelinA3-IL-6complex exhibited both higher energy peaks at initial FEL analysis but showed maximum local minima (14 KJ/mol) at the end. Hence we can say that GibberelinA3-IL-6complex showed stable and firm binding after initial robust energy scattering. Meanwhile, aspindinol-IL-6 complex revealed a moderate rugged energy surface profile with both wider and shallow energy basin, suggesting intermediate stability.

**Binding free energy (MMGBSA) calculations**

The MMGBSA calculations were employed to assess the binding energies of simulated complexes involving gibberelin A3-IL-6, aspidinol-IL6, gibberelin A3-IL-1ß, and ferulic acid-IFN-gamma complexes. The MMGBSA method was employed to calculate the binding free energies including $\Delta G_{bind}$, $\Delta G_{bindCoulomb}$, $\Delta G_{bindCovalent}$, $\Delta G_{bindHbond}$, $\Delta G_{bindLipo}$, $\Delta G_{bindSolvGB}$, and $\Delta G_{bindvdW}$ was calculated. The last 50 frames of the simulation trajectory were selected for analysis. The calculated binding free energy ($\Delta G_{bind}$) was determined as -75.05 kcal/mol for the aspidinol-IL6 complex. This significant negative value suggests a strong binding between ligand and the target protein. Similarly, the gibberelin A3-IL-6complex exhibited a $\Delta G_{bind}$ of -75.05 kcal/mol, indicating a favorable binding affinity. In case of gibberelin A3-IL-1ß complex, the $\Delta G_{bind}$ value was -74.85 kcal/mol, suggestive of a firm and stable binding affinity. . Similarly, ferulic acid-IFN-gamma complex exhibited a $\Delta G_{bind}$ of -74.94 kcal/mol. Hence after comparing the four complexes, it is evident that all complexes exhibits the stronger binding energies, attributed to a stable and firm binding interactions.

Overall, the FEL results with the PCA findings and MD simulation analysis showed that the ferulic acid-IFN-gamma complex was more stable, followed by all three gibberelinA3-IL-1ßcomplex, aspindinol-IL-6 complex and lastly gubberelinA3-IL-6 complex. [43, 46].

The molecular docking and molecular dynamics simulation results collectively suggest that the phytoconstituents of *Dryopteris cochleata* possess promising **immunomodulatory potential** through their stable interactions with key immune-regulating cytokines, including **IL-1β, IL-6, and IFN-γ**. These cytokines play central roles in initiating and regulating innate and adaptive immune responses. Among the investigated compounds, **gibberellin A3** exhibited the strongest interaction with **IL-1β**, while **gibberellin A3, aspidinol, and quercetin** demonstrated favorable binding toward **IL-6**, and **ferulic acid** showed the highest affinity for **IFN-γ**. The binding affinities of these phytochemicals were comparable to or better than the standard immunomodulator, **levamisole**, indicating their potential to regulate cytokine-mediated signaling pathways. Furthermore, MD simulation analyses, including RMSD, RMSF, radius of gyration, SASA, PCA, FEL, and MM/GBSA calculations, confirmed the structural stability of the protein–ligand complexes throughout the 100 ns simulation period. Stable binding with favorable binding free energies (approximately **−75 kcal/mol**) suggests sustained interactions that may influence cytokine function. Since IL-1β and IL-6 are involved in macrophage activation, lymphocyte proliferation, and initiation of inflammatory responses, whereas IFN-γ plays a crucial role in activating macrophages, enhancing antigen presentation, and promoting Th1-mediated cellular immunity, modulation of these cytokines by *D. cochleata* phytoconstituents may contribute to enhancement of host immune responses. Therefore, the computational findings indicate that **gibberellin A3, aspidinol, quercetin, and ferulic acid** are promising immunomodulatory phytochemicals capable of interacting with major immune regulatory proteins, supporting the traditional medicinal use of *Dryopteris cochleata* and warranting further **in vitro** and **in vivo** investigations to validate their immunostimulatory efficacy.

**Acknowledgements**
The authors thank Tatyasaheb Kore College of Pharmacy, Warananagar for supporting this Ph.D research.

**Declaration of competing interest**
The authors declare that they have no conflict of interests.

**Author contributions statement**
**Shubhangi Patil:** Investigation, Data curation, Methodology and Resources, and Writing - original draft and editing; **Popat Kumbhar:** Methodology, Fornal analysis, Writing – reviewing and editing; **Sandeep Kane:** Molecular docking & MD simulation
**John Disouza:** Conceptualization, Supervision, and Writing – reviewing and editing.
**Funding**
No funding was received for this project.
**Data availability statement**
All data and material are made available upon request.

This work is carried as a Ph D research of Shubhangi Patil**References:**

1. Medzhitov R. Origin and physiological roles of inflammation. **Nature.** 2008;454:428–435.
2. Chen L, Deng H, Cui H, et al. Inflammatory responses and inflammation-associated diseases. **Oncotarget.** 2018;9(6):7204–7218.
3. Nathan C, Ding A. Nonresolving inflammation. **Cell.** 2010;140(6):871–882.
4. Dinarello CA. Overview of the IL-1 family in innate inflammation and acquired immunity. **Immunol Rev.** 2018;281(1):8–27.
5. Schett G, Dayer JM, Manger B. Interleukin-1 function and role in disease. **Arthritis Res Ther.** 2016;18:70.
6. Dinarello CA. Immunological and inflammatory functions of the interleukin-1 family. **Annu Rev Immunol.** 2009;27:519–550.
7. Tanaka T, Narazaki M, Kishimoto T. IL-6 in inflammation, immunity and disease. **Cold Spring Harb Perspect Biol.** 2014;6:a016295.
8. Schoenborn JR, Wilson CB. Regulation of interferon-gamma during innate and adaptive immunity. **Adv Immunol.** 2007;96:41–101.
9. Barnes PJ. Anti-inflammatory actions of glucocorticoids. **Clin Sci.** 1998;94:557–572.
10. Rang HP, Ritter JM, Flower RJ, Henderson G. **Rang & Dale's Pharmacology.** 9th ed. Elsevier; 2020.
11. Newman DJ, Cragg GM. Natural products as sources of new drugs. **J Nat Prod.** 2020;83:770–803.
12. Kumar S, Pandey AK. Chemistry and biological activities of flavonoids. **ScientificWorldJournal.** 2013;2013:162750.
13. Singh M, Singh N, Khare PB, Rawat AKS. Phytochemistry and pharmacological potential of *Dryopteris* species: A review. **J Ethnopharmacol.** 2018.
14. Li Y, Yao J, Han C, et al. Quercetin, inflammation and immunity. **Nutrients.** 2016;8:167.
15. Boots AW, Haenen GRMM, Bast A. Health effects of quercetin. **Eur J Pharmacol.** 2008;585:325–337.
16. Na M, Jang J, Min BS, et al. Antimicrobial phloroglucinol derivatives from *Dryopteris* species. **Planta Med.** 2006.
17. Hedden P, Sponsel V. A century of gibberellin research. **J Plant Growth Regul.** 2015;34:740–760.
18. Lionta E, Spyrou G, Vassilatis DK, Cournia Z. Structure-based virtual screening for drug discovery. **Curr Top Med Chem.** 2014;14:1923–1938.

19. Meng XY, Zhang HX, Mezei M, Cui M. Molecular docking: A powerful approach for structure-based drug discovery. **Curr Comput Aided Drug Des.** 2011;7:146–157.
20. Hollingsworth SA, Dror RO. Molecular dynamics simulation for all. **Neuron.** 2018;99:1129–1143.
21. Lipinski CA. Lead- and drug-like compounds: the Rule of Five. **Drug Discov Today Technol.** 2004;1:337–341.
22. Daina A, Michielin O, Zoete V. SwissADME: A free web tool to evaluate pharmacokinetics, drug-likeness and medicinal chemistry friendliness of small molecules. **Sci Rep.** 2017;7:42717.
23. Berman HM, Westbrook J, Feng Z, et al. The Protein Data Bank. **Nucleic Acids Research**. 2000;28(1):235–242.
24. Burley SK, Berman HM, Christie C, et al. RCSB Protein Data Bank: biological macromolecular structures enabling research and education. **Nucleic Acids Research**. 2019;47:D464–D474.
25. Schrödinger Release 2022-1: Protein Preparation Wizard, Schrödinger LLC, New York, NY, USA.
26. Sastry GM, Adzhigirey M, Day T, Annabhimoju R, Sherman W. Protein and ligand preparation: parameters, protocols and influence on virtual screening enrichments. **Journal of Computer-Aided Molecular Design**. 2013;27:221–234.
27. Harder E, Damm W, Maple J, et al. OPLS3: A force field providing broad coverage of drug-like molecules and proteins. **Journal of Chemical Theory and Computation**. 2016;12:281–296.
28. Guex N, Peitsch MC. Swiss-PdbViewer: A fast and easy-to-use protein visualization program. **Electrophoresis**. 1997;18:2714–2723.
29. Kim S, Chen J, Cheng T, et al. PubChem in 2021: new data content and improved web interfaces. **Nucleic Acids Research**. 2021;49:D1388–D1395.
30. Schrödinger Release 2022-1: LigPrep, Schrödinger LLC.
31. Sterling T, Irwin JJ. ZINC 15—Ligand discovery for everyone. **Journal of Chemical Information and Modeling.** 2015;55:2324–2337.
32. Daina A, Michielin O, Zoete V. SwissADME: A free web tool to evaluate pharmacokinetics, drug-likeness and medicinal chemistry friendliness of small molecules. **Scientific Reports**. 2017;7:42717.
33. Daina A, Zoete V. A BOILED-Egg to predict gastrointestinal absorption and brain penetration of small molecules. **ChemMedChem**. 2016;11:1117–1121.
34. Friesner RA, Banks JL, Murphy RB, et al. Glide: A new approach for rapid, accurate docking and scoring. **Journal of Medicinal Chemistry**. 2004;47:1739–1749.
35. Halgren TA. Identifying and characterizing binding sites using SiteMap. **Journal of Chemical Information and Modeling**. 2009;49:377–389.
36. Schrödinger Release 2022-1: Glide, Schrödinger LLC.
37. Meng XY, Zhang HX, Mezei M, Cui M. Molecular docking: A powerful approach for structure-based drug discovery. **Current Computer-Aided Drug Design.** 2011;7:146–157.
38. Bowers KJ, Chow E, Xu H, et al. Scalable algorithms for molecular dynamics simulations on commodity clusters. **Proceedings of SC06**. 2006.
39. Schrödinger Release 2022-1: Desmond Molecular Dynamics System.
40. Jorgensen WL, Chandrasekhar J, Madura JD, et al. Comparison of simple potential functions for simulating liquid water. **Journal of Chemical Physics**. 1983;79:926–935.
41. Hollingsworth SA, Dror RO. Molecular dynamics simulation for all. **Neuron.** 2018;99:1129–1143.
42. Hospital A, Goñi JR, Orozco M, Gelpí JL. Molecular dynamics simulations: advances and applications. **Advances and Applications in Bioinformatics and Chemistry.** 2015;8:37–47.
43. Lipinski CA, Lombardo F, Dominy BW, Feeney PJ. Experimental and computational approaches to estimate solubility and permeability in drug discovery and development settings. **Advanced Drug Delivery Reviews.** 2001;46:3–26.

44. Veber DF, Johnson SR, Cheng HY, et al. Molecular properties influencing oral bioavailability. **Journal of Medicinal Chemistry**. 2002;45:2615–2623.
45. Ghose AK, Viswanadhan VN, Wendoloski JJ. A knowledge-based approach in designing combinatorial libraries. **Journal of Combinatorial Chemistry**. 1999;1:55–68.
**46.** Egan WJ, Merz KM Jr, Baldwin JJ. Prediction of drug absorption using multivariate statistics. **Journal of Medicinal Chemistry**. 2000;43:3867–3877.